



Dempster, T.J., and Macdonald, F. (2016) Controls on fluid movement in crustal lithologies: evidence from zircon in metaconglomerates from Shetland. *Geofluids*, 16(3), pp. 507-517. (doi:[10.1111/gfl.12172](https://doi.org/10.1111/gfl.12172))

This is the author's final accepted version.

There may be differences between this version and the published version. You are advised to consult the publisher's version if you wish to cite from it.

<http://eprints.gla.ac.uk/117403/>

Deposited on: 10 March 2016

Enlighten – Research publications by members of the University of Glasgow
<http://eprints.gla.ac.uk>

Controls on fluid movement in crustal lithologies: evidence from zircon in metaconglomerates from Shetland

Journal:	<i>Geofluids</i>
Manuscript ID	GFL-2015-038.R2
Manuscript Type:	Original Manuscript
Date Submitted by the Author:	n/a
Complete List of Authors:	Dempster, Tim; University of Glasgow, School of Geographical and Earth Sciences Macdonald, Fiona; University of Aberdeen, School of Geosciences
Key words:	zircon, fluids, deformation, permeability, metaconglomerate, quartzite, granite

1
2
3
4
5
6
7
8
9
10
11
12
13
14
15
16
17
18
19
20
21
22
23
24
25
26
27
28
29
30
31
32
33
34
35
36
37
38
39
40
41
42
43
44
45
46
47
48
49
50
51
52
53
54
55
56
57
58
59
60

**Controls on fluid movement in crustal lithologies: evidence from zircon in
metaconglomerates from Shetland**

TIM DEMPSTER* & FIONA MACDONALD¹.
*School of Geographical and Earth Sciences, University of Glasgow, Glasgow G12
8QQ, UK.*

Running title: Monitoring permeability in crustal rocks using zircon textures
Key words: zircon, fluids, permeability, deformation, conglomerate

* Corresponding author: T.J. Dempster, School of Geographical and Earth
Sciences, University of Glasgow, Glasgow G12 8QQ, UK.
Tel: +44 (0) 1413305445
Fax: +44 (0) 1413304817
Email: Tim.Dempster@glasgow.ac.uk

1. Present address: School of Geosciences, University of Aberdeen, Old
Aberdeen AB24 3UE, UK.

ABSTRACT

An investigation of the morphology of zircon in clasts and matrix of a greenschist facies metaconglomerate from Shetland has revealed a history of alteration of radiation-damaged grains, partial dissolution and growth of new zircon. These processes are linked to the generation of chemically modified dark BSE zircon that is spatially related to fractures generated during radiation damage; embayments and rounding of zircon margins; and late overgrowths of original grains. These late modifications of zircon are all linked to the presence of fluids and so zircon morphology is used to track fluid behaviour in different lithologies in the metaconglomerate. Alteration is unrelated to clast margins and radically different in various clast types. This reflects a difference in permeability and suggests that deformation strongly controls fluid influx into quartzite, whereas zircon alteration in granite is associated with a restricted permeability reflecting the more limited response to deformation events.

INTRODUCTION

Fluids in the Earth's crust are important in many respects; they may control mineral reactions, influence deformation processes, facilitate heat transfer and the accumulation of economic resources (Ferry 1984; Bickle & McKenzie 1987; Chamberlain & Rumble 1988; Yardley 2009). The movement of fluids in deep crustal rocks is typically monitored by chemical or isotopic techniques through the analysis of minerals thought to have been in equilibrium with those fluids (Kohn & Valley 1994; Skelton *et al.* 1995; Cartwright 1997; Pitcairn *et al.* 2010). Fluid pathways may be constrained by textural evidence of localized mineral dissolution and new growth (Holness & Watt 2001; Oliver & Bons 2001; Dempster *et al.* 2006). Thus reactive and

1
2
3
4
5
6
7
8
9
10
11
12
13
14
15
16
17
18
19
20
21
22
23
24
25
26
27
28
29
30
31
32
33
34
35
36
37
38
39
40
41
42
43
44
45
46
47
48
49
50
51
52
53
54
55
56
57
58
59
60

soluble phases may be dissolved in one location, components transported within the fluid and re-precipitated in a distal site where conditions are sufficiently different to promote crystallization.

Zircon is present in many common crustal rock types (Harley & Kelly 2007) and has the advantage in regards to monitoring fluid interactions in that in some forms it is very stable (Wilde *et al.* 2001, Kröner, 2010); but in a radiation-damaged state it is exceptionally reactive and prone to alteration in the presence of fluids (Dempster *et al.* 2004; Ramussen 2005; Hay & Dempster 2009a,b). In this damaged and altered state zircon commonly experiences dissolution in hydrous fluids (Ewing *et al.* 1982; Delattre *et al.* 2007; Geisler *et al.* 2007). Local re-precipitation of that reactive zircon in a stable form is favoured by the generally low capacity of hydrous fluids to incorporate high Zr concentrations (e.g. Ayers & Watson 1991). As a consequence, evidence of both dissolution and reprecipitation are typically observed in adjacent areas or within the same crystal. Hence zircon textures can provide information on initial fluid access and scales of fluid migration (Dempster *et al.* 2008b; Dempster & Chung 2013).

In this study we use variations in the morphology of zircon within and between adjacent clasts and matrix to assess controls on fluid movements within metaconglomerates from the island of Fetlar, northeast Shetland, UK.

Metaconglomerates represent a potentially useful rock type to assess lithological controls on fluid distribution as adjacent clasts and matrix may share a common metamorphic history. As such metaconglomerates may represent an ideal test site for variety of petrological processes.

GEOLOGICAL SETTING AND PETROGRAPHY

Samples were collected from two coastal sites on Funzie Ness, in the southeast of Fetlar, Shetland at locations HU65476 88658 and HU66370 89523 (UK Ordnance Survey Grid). The metaconglomerates mapped and documented by Flinn (1956), contain abundant clasts of quartzite, with rarer marble, granite and schist. Clast sizes are typically 10-20 cm long and have been deformed during regional metamorphism such that they are both flattened and elongated within a fine grained phyllite matrix (Fig.1). Clasts typically form >50% of the metaconglomerate throughout the outcrop area. The external fabric anastomoses around the clasts and “pressure shadow” triangular areas are present at the ends of the larger clasts containing fine grained quartz (Fig. 2A). The timing of deformation is uncertain but style of deformation varies slightly with proximity to the faulted contact with the Caledonian Unst ophiolite to the west (Flinn 1956; Flinn & Oglethorpe 2005; Crowley & Strachan 2015). Although the metamorphic grade of the metaconglomerate matrix appears to be identical at both sample sites, overall deformation intensity is slightly lower towards the southwest of the area, at sample site HU65476 88658, with marginally greater elongation of clasts but less constriction (Flinn 1956). Quartzite clasts are dominated by >98% quartz with minor amounts of muscovite (Fig. 2B), biotite, plagioclase, epidote and zircon. Quartz (up to 500 μm by 300 μm) typically shows a well-developed shape fabric (Fig. 2B,C), with bulging recrystallization on the grain boundaries of larger crystals which show subgrain formation. Phyllosilicates are aligned along thin discontinuous anastomosing bands that are parallel to the fabric in the matrix (Fig. 2A). Some variation in the intensity of deformation is shown by the internal shape fabric of the clasts and correlates with average grain size of the quartz (Fig. 2B,C). Muscovite is typically fine grained but individual flakes may occur up to 500 μm (Fig. 2B). Biotite is relatively sparse and

1
2
3
4
5
6
7
8
9
10
11
12
13
14
15
16
17
18
19
20
21
22
23
24
25
26
27
28
29
30
31
32
33
34
35
36
37
38
39
40
41
42
43
44
45
46
47
48
49
50
51
52
53
54
55
56
57
58
59
60

typically unevenly distributed within the quartzite clasts with greater concentrations around the edge of the clast. Locally biotite shows minor alteration to chlorite. Quartz fabrics in the clasts are consistently aligned between individual clasts and sub-parallel to the external fabric in the matrix. Deformation as shown by the quartz fabric may be locally more intense near the edge of the clasts. The clasts show a sharp well defined boundaries with the matrix marked by the consistently coarser grain size of quartz in the former (Fig. 2A)..

Granite clasts are also elongate and slightly flattened, but typically smaller and less obviously strained than those of quartzite. In the unaltered parts of the clasts they contain abundant plagioclase (50%) and quartz (45%) (Fig. 2G,H), together with muscovite and trace amounts of biotite. Fabrics with weak alignment parallel to the foliation of the matrix are present within localised areas of finer grained quartz (Fig. 2H) but are not as strongly developed as within the quartzite clasts. Large (1-2 mm) plagioclase shows less evidence of deformation and may show relict subhedral shapes within a typically recrystallised finer grained quartz matrix (Fig. 2G) in a possible relict interstitial texture. Clusters of coarser grained (100-200 μm) muscovite typically lack alignment. Plagioclase shows patchy alteration within the granite, from sparse sericitization to almost complete alteration to very fine grained phyllosilicates (Fig. 2F). Areas showing the latter may have a slightly more intense fabric with aligned muscovite and biotite. Even at the very edge of granite clasts (Fig. 2F), the fabric within the phyllosilicates is not strongly developed.

The matrix of the metaconglomerate contains mm-thick layers with abundant strongly aligned muscovite and locally biotite and epidote (Fig. 2E). These are interbanded with more quartz-rich layers, some of which may represent highly attenuated small clasts and some original quartz-rich beds (Fig. 2D). Muscovite in the phyllitic layers

1
2
3 is typically fine grained (50-200 μm) although sparse larger 2 mm grains are present
4
5 and these may show evidence of late kinking (Fig. 2E). Clasts of individual quartz and
6
7 plagioclase grains and lithic clasts of granular quartzo-feldspathic rock within the
8
9 matrix typically have a strong shape fabric (Fig. 2E), with beards of white mica and
10
11 local pressure shadows adjacent to the large clasts. The larger individual grains are
12
13 approximately 0.5 - 1 mm diameter. Biotite tends to occur both within aligned clusters
14
15 and sparse larger books with cleavage oriented at high angles to the rock fabric (Fig.
16
17 2F). Locally very fine grained mylonitic layers occur parallel to the fabric in the
18
19 matrix (Fig. 2D). These layers are ca. 2 mm thick with isolated small (<50 μm)
20
21 porphyroclasts of quartz in a muscovite- and epidote-rich matrix.
22
23 The presence of matrix biotite, the grain size of the fabric forming muscovite, and the
24
25 quartz grain boundary textures, all indicate that the metaconglomerate has
26
27 experienced greenschist facies regional metamorphism. Strain is generally
28
29 homogeneous through the bulk of the rock but also localized in some thin mylonitic
30
31 zones within the matrix. Fabrics are typically parallel in the matrix and clasts,
32
33 although some refraction at the edges of the clasts is also present. The quartzite clasts
34
35 have experienced an earlier metamorphism, as evidenced by their larger grain size of
36
37 than the matrix and the sharp nature of the clast boundaries. However there is no
38
39 evidence of any pre-existing alignment associated with that earlier event.
40
41
42
43
44
45
46
47

48 METHODS

49
50 Zircon morphology was characterized using a FEI Quanta 200F field-emission
51
52 environmental scanning electron microscope at the University of Glasgow operated at
53
54 20 kV on polished thin sections of each sample. A total of five polished sections from
55
56 representative clasts were characterized with each section containing a matrix/clast
57
58
59
60

1
2
3
4
5
6
7
8
9
10
11
12
13
14
15
16
17
18
19
20
21
22
23
24
25
26
27
28
29
30
31
32
33
34
35
36
37
38
39
40
41
42
43
44
45
46
47
48
49
50
51
52
53
54
55
56
57
58
59
60

boundary; two polished sections were from granite clasts from sample site HU66370 89523 and three from quartzite clasts from locality HU65476 88658. Thin section petrography of clasts from both sites confirms that those selected are representative. Textural characterization of zircon was achieved through X-ray mapping to locate all zircon grains in each thin section and backscattered electron (BSE) imaging of the individual grains and adjacent matrix phases.

RESULTS

Zircon characteristics

Zircon is particularly abundant within the matrix but also common in both the quartzite and granite clasts. Typically zircon is small with a 5-6 μm average radius (Figs 3 & 4), and a maximum radius of ca. 50 μm is observed. Although rare small ca. 1 μm radius zircons are present, no micro-zircon (cf. Dempster *et al.* 2008a) are present in any of the lithologies examined. Most zircons are equant, and some are euhedral, although zircons in both the quartzite and matrix are characterized by a slightly more rounded appearance than those in the granite clast. About 10% of all zircons show evidence of brittle deformation (Fig. 3A), typically with fragments of the original grain being displaced and dispersed parallel to cleavage in both the quartzite clast (Fig. 3G) and the matrix (Fig. 4F,H,I). Zircon is characterized by a range of alteration textures which may affect the whole grain or be confined to original concentric growth zones (Figs 3 & 4). Radial cracks are commonly present within the zircon (Fig. 4B). Alteration may produce different types, either a dark heterogeneous texture in BSE images (Hay & Dempster 2009a) or a more uniform alteration (Geisler *et al.* 2003; Rayner *et al.* 2005; Geisler *et al.* 2007; Hay & Dempster 2009b). Both types of alteration may be spatially linked to radial cracks

1
2
3 within the original host zircon (Figs 3F,4B). The heterogeneous altered zircon has a
4
5 porous structure with a patchy inclusion-rich appearance (Fig 3D,G). Zircons showing
6
7 this type of alteration are commonly completely altered and altered areas of the zircon
8
9 are typically in contact with surrounding minerals. The more homogeneous type of
10
11 altered dark BSE zircon contains randomly oriented cracks (Fig. 4C), it may replace
12
13 large areas of the original host or may be confined to particular growth zones (Fig.
14
15 3B) and may also form bulbous structures within the host (Fig. 3A). Such altered
16
17 zircons typically retain their original shape (Fig. 4A) better than those with the
18
19 heterogeneous alteration (Fig. 4I). Highly porous light BSE zircon is also present
20
21 (Fig. 3H), and is most abundant in the quartzite clasts. About 10% of the whole zircon
22
23 population contains no dark BSE zircon and are apparently chemically unaltered
24
25 (Figs. 3E,4D). Small overgrowths of either light or dark BSE zircon may also be
26
27 present along the margins of some host zircons forming either isolated tiny ($<1\ \mu\text{m}$)
28
29 pyramidal protrusions from the grain surface (Fig. 3H) or a thicker semi-continuous
30
31 crust around existing grains (Fig. 3C). In some instances, such overgrowths may also
32
33 form on fractured surfaces of the host grain. Rare xenotime is present as overgrowths
34
35 on altered zircon within the quartzite (Fig. 3D). Hence the rocks contain the same low
36
37 temperature zircon assemblages that Hay and Dempster (2009a,b) have reported from
38
39 both slates and sandstones.
40
41
42
43
44
45
46

47 **Characteristics of zircon in the granite clasts**

48
49 A total of 145 zircons were characterized in granite clasts. Generally less zircon is
50
51 present in the areas with coarse grained feldspars and may reflect an original feature
52
53 of the granite. Relatively unaltered zircon is more evenly distributed on the scale of a
54
55 thin section, and the distribution of the highly altered zircon is more clustered.
56
57
58
59
60

1
2
3
4
5
6
7
8
9
10
11
12
13
14
15
16
17
18
19
20
21
22
23
24
25
26
27
28
29
30
31
32
33
34
35
36
37
38
39
40
41
42
43
44
45
46
47
48
49
50
51
52
53
54
55
56
57
58
59
60

Despite these differences there are many instances where unaltered zircon occurs in close proximity to highly altered zircon. The zircons are typically equant, euhedral and overgrowths are only rarely developed (Fig. 5) and when present typically very small ($<1\text{ }\mu\text{m}$). Alteration to dark BSE zircon rarely affects the whole grain and is typically restricted to particular growth zones of the zircon, often in internal areas (Fig. 3B). Some zircons show alteration confined to particular growth zones but alteration fronts may be unrelated to the geometry of those growth zones (Fig. 3A). The proportion of zircon in the granite that lacks any alteration is low (Fig. 6) and the average amount of alteration in the zircon in the granite clast is high. Higher proportions of altered zircon occur next to quartz and plagioclase than adjacent to muscovite. Alteration typically produces homogeneous dark BSE zircon, with only 4% of the zircons showing exclusively heterogeneous alteration (Fig. 7). No porous light BSE zircon is present in the granite clast. 8% of the zircons in the granite show evidence of deformation. The alteration of zircon shows no systematic relationship to proximity to the edge of the clast (Fig. 8).

Characteristics of zircon in the quartzite clasts

A total of 175 zircons were characterized in the quartzite clasts. The quartzite contains generally equant slightly rounded zircons. A few euhedral grains are present and these are typically small unaltered and enclosed within single grains of quartz (Fig. 3E). Complex overgrowths are present on some zircons (Fig. 3C). Many grains with high degrees of dark BSE alteration are present (Fig. 6) and these typically have irregular margins (Fig. 3D, G). The quartzite clasts contain high proportions of the most altered zircon but also high proportions of virtually unaltered zircon (Fig. 6). The alteration of zircon and the abundance of overgrowths in the quartzite clasts are independent of

the proximity to the clast edge (Fig. 8). Heterogeneous dark BSE alteration is dominant (Fig. 7) and porous light BSE zircon (Fig. 3H) is also relatively abundant. Radial fractures are common within zircon even in those lacking dark BSE zircon. 14% of zircons show evidence of break-up and brittle deformation, this is particularly associated with some of the most highly altered zircon (Fig. 3G). Typically fracturing is associated with minor displacements and quartz infills the fractures. Overgrowths are larger and higher proportions of alteration occur adjacent to muscovite than adjacent to quartz (Fig. 8). Given the relative paucity of micas within the quartzite clasts (<1%) a high proportion of zircons (ca. 40%) are adjacent to phyllosilicates. 19% of zircons contain a proportion of porous structure (Fig. 7) and 82% of these are adjacent to quartz. Porous zircon rarely occurs next to muscovite and those that do are typically partly altered to heterogeneous dark BSE zircon (Fig. 3G).

Characteristics of zircon in the metaconglomerate matrix

A total of 516 zircons were examined from the matrix. These are from a range of different textural sites, including: the phyllosilicate-rich phyllite layers; a thin mylonite; quartz-rich layers; and, quartz-rich patches within the “pressure shadow” areas at the ends of elongate clasts. Zircons in the matrix are of similar size to those in clasts. 18% of zircons in the matrix show evidence of deformation and displacement along fractures, with grains broken up and dispersed along the line of the cleavage (Fig. 4F). Such fractured zircon typically has subrounded crystal edges and there is a lack of small angular fragments associated with the brittle deformation (Fig. 4H,J). A few small euhedral zircon are present (Fig. 4D). Overgrowths are both large and abundant on zircon in the matrix (Fig. 4E,G). The mylonite bands within the matrix contain the highest proportions of zircon overgrowths (Fig. 5). Altered grains are

1
2
3
4
5
6
7
8
9
10
11
12
13
14
15
16
17
18
19
20
21
22
23
24
25
26
27
28
29
30
31
32
33
34
35
36
37
38
39
40
41
42
43
44
45
46
47
48
49
50
51
52
53
54
55
56
57
58
59
60

abundant but overall proportions of alteration are relatively low and 60% of zircon grains show <10% alteration (Fig. 6). Alteration and the formation of overgrowths are both more common in zircons adjacent to phyllosilicates rather than quartz (Fig. 9). Heterogeneous alteration very commonly occurs in zircon next to muscovite and such zircon also shows most evidence of deformation. Porous zircon is uncommon in the matrix (Fig. 7). Homogeneous alteration of zircon is dominant in the matrix (Fig. 7) and such alteration is most frequently confined within cores or growth zones. As such these zircons tend to have more euhedral forms. Dark homogeneous BSE zircon that is within the internal parts of the grain is linked to fluid access along radial cracks in the outer parts of the grain (Fig. 4B). Those grains showing heterogeneous alteration typically have very irregular margins, and frequently have major embayments and show partial replacement by quartz (Fig. 4I).

Variations between clasts and matrix and between different clast types

Typically less alteration is observed in the matrix zircons, which are characterized by few grains with very high proportions of alteration and many with no evidence of alteration (Fig. 6). The matrix zircons also show the most evidence of deformation and the textures of both altered and fractured grains indicate that significant dissolution of both altered and unaltered zircon has occurred. Overgrowths are both more abundant and larger on zircons in the matrix than those in either clast type (Fig. 5). Homogeneous alteration is dominant in the matrix zircon and very few porous zircons are present (Fig. 7). Both alteration and new growth of zircon appears to be favoured by proximity to muscovite (Fig. 9). The largest differences between zircon types present are those between zircons in the granite and quartzite clasts. Those within quartzite are characterized by intermediate

proportions of altered zircon, but abundant highly altered grains, and relatively rare overgrowths. Alteration is dominated by heterogeneous grains, and, relative to other parts of the metaconglomerate, chemically unmodified porous zircon is abundant (Fig. 7). Given the overall low proportion of muscovite present within the quartzite clasts many zircons are adjacent to muscovite grains. Those zircons adjacent to muscovite within the quartzite, are much more likely to have overgrowths and show alteration (Fig. 9). In contrast to the other forms of alteration, a far lower proportion of porous zircon occurs adjacent to muscovite.

The granite clast is dominated by homogeneous alteration of zircon, and no porous zircon is present (Fig. 7). Although the average amount of alteration is highest within the granite clast, very few zircons are completely altered, very few are completely unaltered (Fig. 6) and very few overgrowths are present (Fig. 5). The parts of the granite clast with more sericitization of plagioclase typically contain slightly less altered zircon and may have fewer overgrowths.

INTERPRETATION

Zircon Textures

The interpretation of the textures of zircon follows earlier publications on low temperature zircon morphology (e.g. Hay & Dempster 2009a):

Light BSE zircon represents chemically unmodified zircon (e.g. Fig 3E).

Fractured zircon occurs in two types: Radial or less commonly concentric fractures that are spatially linked to growth zones in the host grain are associated with volume changes in the lattice of the zircon due to radiation damage (Lee & Tromp 1995) (e.g. Fig. 4B). Fractures with large displacements are unrelated to internal zoning structure of the zircon and are associated with deformation events (e.g. Fig. 4J).

1
2
3
4
5
6
7
8
9
10
11
12
13
14
15
16
17
18
19
20
21
22
23
24
25
26
27
28
29
30
31
32
33
34
35
36
37
38
39
40
41
42
43
44
45
46
47
48
49
50
51
52
53
54
55
56
57
58
59
60

Porous zircon has a modified structure but a light BSE signature that indicates a lack of chemical change. These are interpreted as recovery of zircon from a metamict state that have been isolated from fluids. Evidence for radiation damage having caused the structural modification is manifested by radiation related fractures (e.g. Fig. 3H).

Overgrowths of newly formed zircon that may have little relationship to the structural state of the host grain (e.g. Fig. 3C) suggests significant redistribution of Zr and mobility within a fluid phase.

Embayment of zircon margins and rounding of the edges of fragments implies dissolution of the host grain. This is most obvious where deformation related fracturing has occurred and there is an absence of angular edges or small fragments of zircon (e.g. Fig. 4I).

Dark BSE zircon is chemically modified and represents fluid access to structurally modified grains. Typically evidence of fluid access along radiation damage-related fractures is observed. Alteration occurs in two distinct forms:

Heterogeneous altered zircon is thought to form through a dissolution and reprecipitation mechanism (Geisler *et al.* 2007) in a high permeability environment with ready access to fluids. Such zircon is known to have a nanocrystalline structure and is most typically found in low-grade metamorphic environments (Hay & Dempster 2009a). Porous zircon and heterogeneous altered zircon, which itself has a porous structure, are frequently observed within the same grain suggesting that the former alter to produce the latter (e.g. Fig. 3G).

Homogeneous altered zircon may form as a result of in-situ diffusion driven structural recovery (Geisler *et al.* 2004; 2007). Although this recrystallisation must occur in the presence of fluid, it represents more of a closed system with restricted access to fluid and hence a lower permeability and higher levels of Zr saturation in the

fluid. It is known to have a microcrystalline structure (Hay & Dempster 2009b) lacking inclusions and it is notable that this type of alteration is often restricted to internal zones or patches within the host grain (e.g. Fig. 3B) and as such may be less prone to subsequent dissolution than the heterogeneous altered forms. Such altered zircon has previously been observed to form in low temperature sedimentary environments (Hay & Dempster 2009b).

Timing of Zircon Alteration

Many of the alteration and overgrowth characteristics of zircon in both the quartzite and matrix are influenced by the adjacent mineralogy (Fig. 9). This spatial association is controlled by the in-situ deformation and metamorphic conditions. Hence the timing of much of the zircon alteration and formation of any overgrowths is either associated with, or post-dates, the metamorphic event. The evidence from the grain size of the quartzite clasts suggests that they were initially quartzite, not sandstone clasts. However the flattening of the clasts themselves and the mineral alignment within the clasts appears to be entirely related to the deformation of the conglomerate. There is no evidence of an earlier deformation event in the clasts. The relationship between zircon alteration and deformation is less clear-cut in the granite clasts due to the lack of a consistent penetrative metamorphic fabric. The presence of similar zircon alteration textures in the granite clast to those in the matrix suggests that most of the alteration of zircon in the granite may also post-date the sedimentary history of the clast. The nature of the alteration to zircon in all the lithologies that have been studied is also compatible with greenschist facies metamorphism of the conglomerate (Hay & Dempster 2009a).

1
2
3
4
5
6
7
8
9
10
11
12
13
14
15
16
17
18
19
20
21
22
23
24
25
26
27
28
29
30
31
32
33
34
35
36
37
38
39
40
41
42
43
44
45
46
47
48
49
50
51
52
53
54
55
56
57
58
59
60

The zircon population in the matrix may come from a variety of different sources, some may represent disaggregated quartzite and granite and some from other sources, although the abundance of zircon does not suggest a major contribution from ophiolitic material (*cf.* Flinn & Oglethorpe 2005). The generally rounded shape of the relatively unaltered zircon in the matrix is compatible with a detrital origin and those in a highly altered state would be unlikely to survive transportation in a high energy sedimentary environment. This also suggests that any subsequent alteration of zircon within the matrix that is linked to the build up of radiation damage is likely to significantly post-date the sedimentary history. Consequently although there is uncertainty as to the exact timing of zircon alteration it is thought likely that a high proportion of the alteration occurred during the later stages of the evolution of the metaconglomerate rather than early sedimentary processes.

Initial zircon populations in the various clasts and matrix may be different. However, virtually all of the zircons irrespective of their location in the rocks are prone to subsequent alteration. Many of those that show no chemical modification typically do show either a porous structure or contain radiation-damage related cracks (Lee & Tromp 1995) that suggest they have experienced structural modification. As such it is suggested that the only reason that some zircons show little or no chemical modification is due to a lack of interaction with fluids. Given that zircons with both types of alteration are present in overall similar proportions, the alteration type is unlikely to be controlled by temperature (*cf.* Hay & Dempster 2009b). The metamict state of the original grain is also not a dominant control (Hay & Dempster 2009b) but the alteration type is a reflection of the differing response to fluid access.

Consequently the presence or absence of chemical alteration and indeed the type of alteration are all potential proxies for monitoring fluid pathways or local fluid

composition. Although the latter is known to control zircon solubility (Ayers *et al.* 2012; Wilke *et al.* 2012), given the similar buffering mineral assemblages in each of the different lithologies the fluids may be of similar composition.

Fluid Movements

The zircon in the matrix shows abundant evidence of dissolution and this suggests that fluid was pervasively present in the matrix whilst access more was restricted in the clasts. Dissolution of altered zircon in the matrix, especially heterogeneous altered zircon, results in preferential concentration of homogeneous altered zircon. The dissolution of altered or metamict zircon will raise Zr contents in the fluid. This may be synchronous with growth of new zircon lacking radiation damage or alteration that will have lower solubility and so may precipitate as overgrowths from the same fluid. A coupled dissolution-precipitation process may occur on the scale of single grains (Geisler *et al.* 2007) or on a larger scale involving precipitation remote from the zircon undergoing dissolution. Accurate mass balance associated with this dissolution-reprecipitation process is impossible because of uncertainty surrounding original abundance of zircon types in each host lithology. However the very small size of overgrowths in comparison to the size of the host grains coupled to the significant differences in zircon types in each lithology suggests that the dissolution and regrowth of zircon is not a closed system. Overall fewer overgrowths are present than expected from the potential volume of dissolution of heterogeneous zircon, and hence for significant parts of the dissolution-regrowth history the scale of mobility exceeds the scale of the sample. The distribution of overgrowths in the matrix is patchy and most abundant within the mylonite zone. This implies that unless factors such as alkali/Al ratios of fluids (Wilke *et al.* 2012) are of very local composition, zircon precipitation

1
2
3
4
5
6
7
8
9
10
11
12
13
14
15
16
17
18
19
20
21
22
23
24
25
26
27
28
29
30
31
32
33
34
35
36
37
38
39
40
41
42
43
44
45
46
47
48
49
50
51
52
53
54
55
56
57
58
59
60

is controlled by permeability contrasts within the matrix and hence overgrowth distribution may define fluid pathways. Such pathways have been observed using the distribution of microzircon, which may define zones of transient hydrofracturing in greenschist facies metasedimentary rocks (Dempster & Chung 2013).

The zircon in granite and quartzite clasts both show similar overall levels of alteration and so may be equally prone to fluid-related modification, however the styles of alteration are different. Heterogeneous dark BSE altered zircon dominates the population in the quartzite and appears to be typical of low grade metamorphic settings (Hay & Dempster 2009a). This would be consistent with more open system behaviour in the quartzite than within the granite clasts (Hay & Dempster 2009b). Such behaviour may reflect the more pervasive fabric in the quartzite and importance of deformation as a control on fluid access in the metamorphic realm. Zircon alteration, dissolution and overgrowths are all strongly linked to the sparse muscovite in the quartzite clasts. Quartz-mica boundaries may provide sites for preferential fluid access due to anisotropic strain (Hippertt 1994). Chemically unaltered zircon is typically isolated within quartz, and the presence of abundant porous zircon within the quartzite clasts also suggests that there are many structural settings that have remained isolated from fluids. The lack of spatial controls on the alteration process that are linked to the margin of either clast type is striking (Fig. 8), hence fluid access does not represent a diffusive infiltration controlled by proximity to the clast margins but is linked to an irregular network of pathways. As such fluid access in the quartzite appears to be channeled along foliation planes.

Despite the abundant petrographic evidence of sericitization of feldspar within the granite clasts there is a lack of zircon overgrowths or evidence of dissolution and hence limited redistribution of Zr. Homogeneous alteration of zircon is common

1
2
3 within the granite, suggesting that fluids are available on most grain boundaries but
4
5 that permeability is typically restricted. The dominance of homogeneous alteration of
6
7 zircon implies that scales of transport during dissolution-reprecipitation are very small
8
9 scale and hence that there is a lack of effective fluid pathways into these clasts,
10
11 perhaps equivalent to static fluid diffusion metasomatic processes (Korzhinskii 1970).
12
13 This interpretation is supported by evidence for “stalled” alteration within some zones
14
15 prone to alteration (Fig. 3A). Large feldspars in the granite may provide a rigid
16
17 framework (Tullis & Yund 1987), and limit penetrative deformation in these
18
19 greenschist facies rocks. The fact that less alteration occurs in zircon adjacent to
20
21 muscovite in the granite suggests that feldspar replacement reactions may limit
22
23 permeability (Moore *et al.* 1983) and hence zircon alteration. Such contrasts in
24
25 behaviour between zircon adjacent to muscovite in the granite and quartzite clasts also
26
27 point towards a dominant structural influence of the mineralogy rather than local
28
29 controls of fluid composition. Fluid consumption in the feldspar breakdown reaction
30
31 may act to generally reduce fluid availability within the granite. Although fine grained
32
33 alteration products do provide numerous grain boundaries and potential fluid
34
35 pathways, these are not preferentially utilized for subsequent fluid access associated
36
37 with zircon alteration. This suggests that active deformation is the key process
38
39 allowing fluid access rather than infiltration along grain boundaries and hence the
40
41 nature and abundance of those grain boundaries is not a crucial factor.
42
43
44
45
46
47
48
49

50 DISCUSSION

51
52 Fluids are increasingly recognized as important in all reactions and metamorphic
53
54 processes (Putnis & Austrheim, 2010), and this study has shown that their influence
55
56 crucially depends on deformation allowing fluids access to grain boundaries even
57
58
59
60

1
2
3
4
5
6
7
8
9
10
11
12
13
14
15
16
17
18
19
20
21
22
23
24
25
26
27
28
29
30
31
32
33
34
35
36
37
38
39
40
41
42
43
44
45
46
47
48
49
50
51
52
53
54
55
56
57
58
59
60

those lacking abundant fabric forming minerals. Other workers have shown that porosity and permeability may be controlled by mineralogy (Arghe *et al.* 2011; Ferry *et al.* 2013), and equilibrium wetting angles (Holness 1993; Price *et al.* 2004), but there are many reports of a structural control of fluid pathways (e.g. Skelton *et al.* 1995; Abart *et al.* 2002; Pitcairn *et al.* 2010; Kleine *et al.* 2014). Zircon morphology provides a sensitive monitor of fluid pathways in crustal rocks capable of recording a range of different interactions.

Quartzite permeability is strongly controlled by active deformation creating transient fluid pathways. Creep cavitation (Fusseis *et al.* 2009) provides a mechanism for driving fluids along grain boundaries of deforming clasts. The transient permeability of quartzite suggests that few lithologies are impermeable during deformation, although this will be constrained by the conditions that control the structural response. Hence permeability is restricted in granite by a combination of the strength of the feldspar dominated structural framework in the greenschist facies conditions together with feldspar-breakdown, water-consuming reactions that reduce porosity and create an apparent barrier to fluid movement. However the granite may have a more permeable response at higher temperatures (Rosenberg & Stünitz 2003). Muscovite presence appears to act as a general barrier to fluid flow in the granite, but during penetrative deformation it enhances fluid access in the quartzite. The response of minerals to deformation is an important factor in allowing fluid access and it appears that phyllosilicates are primary influences in controlling metamorphic equilibration (Dempster & Tanner 1997) from both a structural and chemical perspective.

Permeability will reflect a complex interplay between fluid consumption and generation, and the differential response of lithologies to deformation.

ACKNOWLEDGEMENTS

This research was supported by the University of Glasgow. Peter Chung and John Gilleece are thanked for technical support. Alasdair Skelton and Bruce Yardley are thanked for their thoughtful reviews of the manuscript.

REFERENCES

- Abart R, Badertscher N, Burkhard M & Povoden E (2002) Oxygen, carbon and strontium isotope systematics in two profiles across the Glarus thrust: implications for fluid flow. *Contributions to Mineralogy and Petrology*, **143**, 192-208.
- Arghe F, Skelton A & Pitcairn I (2011) Spatial coupling between spilitization and carbonation of basaltic sills in SW Scottish Highlands: evidence of a mineralogical control of metamorphic fluid flow. *Geofluids* **11**, 245-259.
- Ayers JC & Watson EB (1991) Solubility of apatite, monazite, zircon, and rutile in supercritical aqueous fluids with implications for subduction zone geochemistry. *Philosophical Transactions of the Royal Society of London (A)*, **335**, 365-375.
- Ayers JC, Zhang L, Luo, Y & Peters TJ (2012) Zircon solubility in alkaline aqueous fluids at upper crustal conditions. *Geochimica et Cosmochimica Acta*, **96**, 18-28.
- Bickle MJ & McKenzie DP (1987) The transport of heat and matter by fluids during metamorphism. *Contributions to Mineralogy and Petrology*, **95**, 384-392.
- Cartwright I (1997) Permeability generation and resetting of tracers during metamorphic fluid flow: implications for advective-dispersion models. *Contributions to Mineralogy and Petrology* **129**, 198-208.
- Chamberlain CP & Rumble D (1988) Thermal anomalies in a regional metamorphic terrane: an isotopic study of the role of fluids. *Journal of Petrology*, **29**, 1215-1232.

- Crowley QG & Strachan RA (2015) U-Pb zircon constraints on obduction initiation of the Unst Ophiolite: and oceanic core complex in the Scottish Caledonides? *Journal of the Geological Society, London*, **172**, 279-282.
- Delattre S, Utsunomiya S, Ewing RC, Boeglin J-L, Braun J-J, Balan E & Calas G (2007) Dissolution of radiation-damaged zircon in lateritic soils. *American Mineralogist*, **92**, 1978-1989.
- Dempster TJ, Campanile D & Holness MB (2006) Imprinted textures on apatite: a guide to paleoporosity and metamorphic recrystallisation. *Geology*, **34**, 897-900.
- Dempster TJ & Chung P (2013) Metamorphic zircon: tracking fluid pathways and the implications for the preservation of detrital zircon. *Journal of the Geological Society*, **170**, 631-639.
- Dempster TJ, Hay DC & Bluck BJ (2004) Zircon growth in slate. *Geology*, **32**, 221-224.
- Dempster TJ, Hay DC, Gordon SH & Kelly NM (2008a) Micro-zircon: origin and evolution during metamorphism. *Journal of Metamorphic Geology*, **26**, 499-507.
- Dempster TJ, Martin JC & Shipton ZK (2008b) Zircon dissolution in a ductile shear zone, Monte Rosa granite gneiss, northern Italy. *Mineralogical Magazine*, **74**, 971-986.
- Dempster TJ & Tanner PWG (1997) The biotite isograd, Central Pyrenees: a deformation - controlled reaction. *Journal of Metamorphic Geology*, **15**, 531-54
- Ewing RC, Haaker RF & Lutze W (1982) Leachability of zircon as a function of alpha dose. In: Lutze W (ed) Scientific basis for radioactive waste management V, Elsevier, Amsterdam, pp 3899-397.
- Ferry JM (1984) A biotite isograd in south-central Maine, U.S.A.: mineral reactions, fluid transfer, and heat transfer. *Journal of Petrology*, **25**, 871-893.

- Ferry JM, Winslow NW & Penniston-Dorland SC (2013) Re-evaluation of infiltration-driven regional metamorphism in northern New England: New transport models with solid solution and cross-layer equilibration of fluid composition. *Journal of Petrology*, **54**, 2455-2485
- Flinn D (1956) On the deformation of the Funzie conglomerate, Fetlar, Shetland. *Journal of Geology*, **64**, 480-505.
- Flinn, D. & Oglethorpe, R.J.D. (2005) A history of the Shetland Ophiolite Complex. *Scottish Journal of Geology*, **41**, 141-148.
- Fusseis F, Regenauer-Lieb K, Liu J, Hough RM & De Carlo F (2009) Creep cavitation can establish a dynamic granular fluid pump in ductile shear zones. *Nature*, **459**, 974-977
- Geisler T, Pidgeon RT, Kurtz R, van Bronswijk W & Schleicher H (2003) Experimental hydrothermal alteration of partially metamict zircon. *American Mineralogist*, **88**, 1496- 1513.
- Geisler T, Schaltegger U. & Tomaschek F (2007) Re-equilibration of zircon in aqueous fluids and melts. *Elements*, **3**, 43-50.
- Geisler T, Seydoux-Guillaume A-M, Wiedenbeck M, Wirth R, Berndt J, Zhang M, Milhailova B, Putnis A, Salje EKH & Schlüter J (2004) Periodic precipitation pattern formation in hydrothermally treated metamict zircon. *American Mineralogist*, **89**, 1341-1347.
- Harley SL & Kelly NM (2007) Zircon tiny but timely. *Elements*, **3**, 13-18.
- Hay DC & Dempster TJ (2009a) Zircon behaviour during low temperature metamorphism. *Journal of Petrology*, **50**, 571-589.
- Hay DC & Dempster TJ (2009b) Zircon alteration, formation and preservation in sandstones. *Sedimentology*, **56**, 2175-2191.

1
2
3
4
5
6
7
8
9
10
11
12
13
14
15
16
17
18
19
20
21
22
23
24
25
26
27
28
29
30
31
32
33
34
35
36
37
38
39
40
41
42
43
44
45
46
47
48
49
50
51
52
53
54
55
56
57
58
59
60

Hippertt JFM (1994) Grain boundary microstructures in micaceous quartzite: Significance for fluid movement and deformation processes in low metamorphic grade shear zones. *Journal of Geology*, **102**, 331-348.

Holness MB (1993) Temperature and pressure dependence of quartz-aqueous fluid dihedral angles: the control of adsorbed H₂O on the permeability of quartzites. *Earth and Planetary Science Letters*, **117**, 363-377.

Holness MB & Watt GR (2001) Quartz recrystallisation and fluid flow during contact metamorphism: A cathodoluminescence study. *Geofluids*, **1**, 215-228.

Kleine BI, Skelton ADL, Huet B & Pitcairn IK (2014) Preservation of Blueschist-facies Minerals along a Shear Zone by Coupled Metasomatism and Fast-flowing CO₂- bearing Fluids. *Journal of Petrology*, **55**, 1905-1939.

Kohn MJ & Valley JW (1994) Oxygen isotope constraints on metamorphic fluid flow, Townshead Dam, Vermont, USA. *Geochimica et Cosmochimica Acta*, **58**, 5551-5568.

Korzhinskii DS (1970) Theory of metasomatic zoning. Oxford University Press, Oxford.

Kröner A (2010) The role of geochronology in understanding continental evolution. *Geological Society, London, Special Publication*, **338**, 179-196.

Lee JKW & Tromp J (1995) Self-Induced fracture generation in zircon. *Journal of Geophysical Research-Solid Earth*, **100**, 17753-17770.

Moore DE, Morrow CA & Byerlee JD (1983) Chemical reactions accompanying fluid flow through granite held in a temperature gradient. *Geochimica et Cosmochimica Acta*, **47**, 445-453.

- Oliver NHS & Bons PD (2001) Mechanisms of fluid flow and fluid-rock interactions in fossil metamorphic hydrothermal systems inferred from vein-wallrock patterns, geometry and microstructure. *Geofluids*, **1**, 137-162.
- Pitcairn IK, Skelton ADL, Broman C, Arghe F & Boyce A (2010) Structurally focused fluid flow during orogenesis: the Islay Anticline, SW Highlands, Scotland. *Journal of the Geological Society, London*, **167**, 659-674.
- Price JD, Wark DA, & Watson BE (2004) Grain-scale permeabilities of synthetic quartzite with volumetrically minor phlogopite, corundum, or aluminosilicate. *Earth and Planetary Science Letters*, **227**, 491-504.
- Putnis A & Austrheim H (2010) Fluid - induced processes: metasomatism and metamorphism. *Geofluids*, **10**, 254-269
- Rasmussen B (2005) Zircon growth in very low grade metasedimentary rocks: evidence for zirconium mobility at similar to 250°C. *Contributions to Mineralogy and Petrology* 150, 146-155.
- Rayner N, Stern RA & Carr D (2005) Grain-scale variations in trace element composition of fluid-altered zircon, Acasta Gneiss Complex, northwestern Canada. *Contributions to Mineralogy and Petrology*, **148**, 721-734.
- Rosenberg CL & Stünitz H (2003) Deformation and recrystallization of plagioclase along a temperature gradient: an example from the Bergell tonalite. *Journal of Structural Geology*, 25, 389-408.
- Skelton ADL, Graham CM & Bickle MJ (1995) Lithological and structural controls on regional 3-D fluid flow patterns during greenschist facies metamorphism of the Dalradian of the SW Scottish Highlands. *Journal of Petrology*, **36**, 563-586.
- Tullis J & Yund RA (1987) Transition from cataclastic flow to dislocation creep of feldspar: mechanisms and microstructures. *Geology*, **15**, 606-609.

1
2
3
4
5
6
7
8
9
10
11
12
13
14
15
16
17
18
19
20
21
22
23
24
25
26
27
28
29
30
31
32
33
34
35
36
37
38
39
40
41
42
43
44
45
46
47
48
49
50
51
52
53
54
55
56
57
58
59
60

Wilde SA, Valley JW, Peck WH & Graham CM (2001) Evidence from detrital zircons for the existence of continental crust and ocean on the Earth 4.4 Gyr ago. *Nature*, **409**, 175-177.

Wilke M, Schmidt C, Dubrill J, Appel K, Borchert M, Kvashnina K & Manning CE (2012) Zircon solubility and zirconium complexation in $H_2O + Na_2O + SiO_2 \pm Al_2O_3$ fluids at high pressure and temperature. *Earth and Planetary Science Letters*, **349**, 15-25.

Yardley BWD (2009) The role of water in the evolution of the continental crust. *Journal of the Geological Society, London*, **166**, 585-600.

FIGURE CAPTIONS

Fig. 1. Field photograph of the Fetlar metaconglomerate. Aligned flattened and elongated clasts in phyllitic matrix. Hammer head is 12cm long.

Fig. 2. Photomicrographs in crossed polarized light. (A) Quartzite clast in matrix (FZ88.1.2) showing clast matrix boundary with strong fabric in matrix and quartz-rich matrix to the right of the clast in a pressure shadow like zone; (B) Interior of quartzite clast (FZ88.1.1) showing fabric and sparse muscovite with high interference colours and sutured boundaries of quartz; (C) Quartzite matrix boundary (FZ88.4) showing alignment of within quartzite and fine grained muscovite-rich matrix; (D) Matrix area (FZ88.4) showing fine grained dark mylonite band in upper right hand area within aligned quartz-rich area of matrix; (E) Muscovite-rich matrix area (FZ88.4) showing large deformed muscovite with fine grained aligned muscovite and quartz and plagioclase porphyroclasts; (F) Contact between muscovite- and biotite-rich matrix (lower right) and altered granite clast (FZ89.4.1) in which plagioclase has been

largely altered to fine grained muscovite. Original quartz has recrystallized to fine grainsize; (G) Largely unaltered central part of granite clast (FZ89.4.2) containing large plagioclase grains in finer recrystallised matrix; (H) Partially altered granite from centre of clast (FZ89.4.2) showing muscovite alteration along edges of plagioclase and adjacent recrystallized quartz.

Fig. 3. Representative backscattered electron (BSE) images of zircons from clasts (A-B: Granite clast; C-H: Quartzite clast). (A) Homogeneous alteration along growth zones with bulbous patchy alteration in core areas; (B) Homogeneous alteration along growth zones with minor dissolution on right edge; (C) Largely unaltered core with large zircon overgrowth; (D) Heterogeneous altered zircon with xenotime overgrowths; (E) Small unaltered euhedral zircon; (F) Homogeneous alteration of growth zones in the core area with larger area of heterogeneous alteration in surrounding area; (G) Porous zircon with patches of heterogeneous alteration; (H) Porous chemically unmodified zircon.

Fig. 4. Representative backscattered electron (BSE) images of zircons from matrix. (A) Homogeneous alteration of internal growth zones; (B) Patchy homogeneous alteration of core area with radial cracking of rim allowing fluid access; (C) Extensive homogeneous alteration; (D) Small unaltered euhedral zircon; (E) Porous zircon with large overgrowths; (F) Fractured zircon with lack of small angular fragments; (G) Largely unaltered zircon with overgrowths; (H) Heterogeneous alteration of zircon with evidence of dissolution (rounding of fragments) and dispersal parallel to rock cleavage; (I) Heterogeneous alteration with large embayments associated with dissolution and replacement by quartz; (J) Homogeneous alteration with evidence of

1
2
3
4
5
6
7
8
9
10
11
12
13
14
15
16
17
18
19
20
21
22
23
24
25
26
27
28
29
30
31
32
33
34
35
36
37
38
39
40
41
42
43
44
45
46
47
48
49
50
51
52
53
54
55
56
57
58
59
60

deformation and dissolution.

Fig. 5. Histogram showing the proportion of zircons with overgrowths in each lithology.

Fig. 6. Histogram showing the amount of alteration of zircon in different host lithologies.

Fig. 7. Histogram showing the proportions of different altered zircon types within each lithology.

Fig. 8. Plots showing relationship between the amount of alteration in individual zircon grains and their proximity to the clast margin for A. Quartzite clasts and B. Granite clasts.

Fig. 9. Histograms showing the influence of adjacent mineralogy on A. the area of alteration in the zircon and B. the area of overgrowth around the zircon.



Fig. 1. Field photograph of the Fetlar metaconglomerate. Aligned flattened and elongated clasts in phyllitic matrix. Hammer head is 12cm long.
209x296mm (150 x 150 DPI)

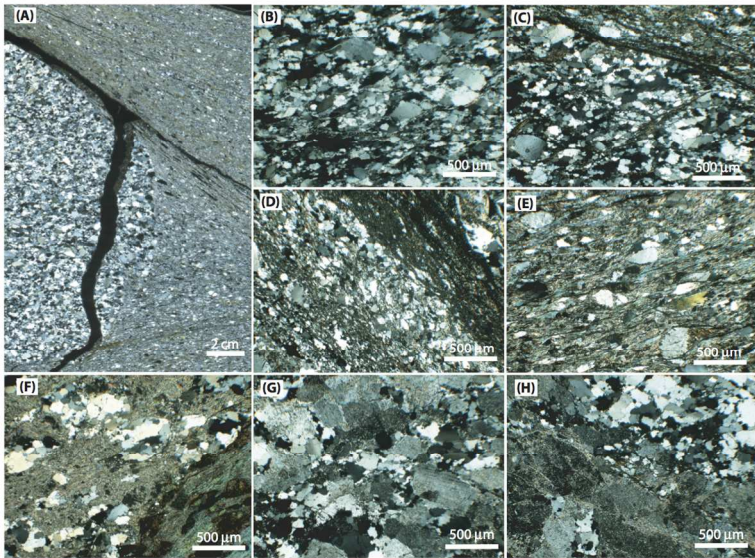


Fig. 2. Photomicrographs in crossed polarized light. (A) Quartzite clast in matrix (FZ88.1.2) showing clast matrix boundary with strong fabric in matrix and quartz-rich matrix to the right of the clast in a pressure shadow like zone; (B) Interior of quartzite clast (FZ88.1.1) showing fabric and sparse muscovite with high interference colours and sutured boundaries of quartz; (C) Quartzite matrix boundary (FZ88.4) showing alignment of within quartzite and fine grained muscovite-rich matrix; (D) Matrix area (FZ88.4) showing fine grained dark mylonite band in upper right hand area within aligned quartz-rich area of matrix; (E) Muscovite-rich matrix area (FZ88.4) showing large deformed muscovite with fine grained aligned muscovite and quartz and plagioclase porphyroclasts; (F) Contact between muscovite- and biotite-rich matrix (lower right) and altered granite clast (FZ89.4.1) in which plagioclase has been largely altered to fine grained muscovite. Original quartz has recrystallized to fine grainsize; (G) Largely unaltered central part of granite clast (FZ89.4.2) containing large plagioclase grains in finer recrystallised matrix; (H) Partially altered granite from centre of clast (FZ89.4.2) showing muscovite alteration along edges of plagioclase and adjacent recrystallized quartz.

296x247mm (150 x 150 DPI)

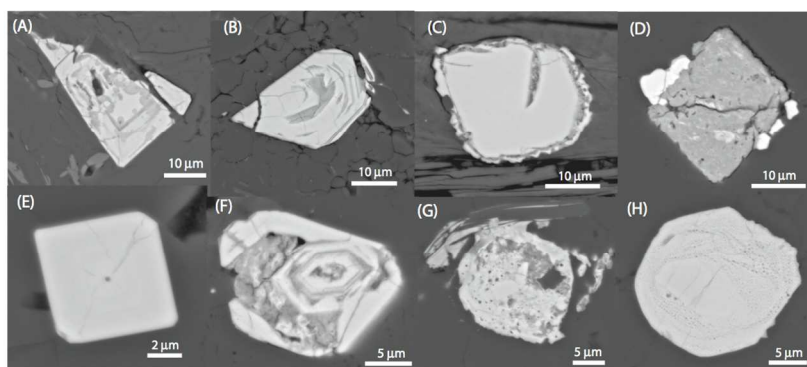


Fig. 3. Representative backscattered electron (BSE) images of zircons from clasts (A-B: Granite clast; C-H: Quartzite clast). (A) Homogeneous alteration along growth zones with bulbous patchy alteration in core areas; (B) Homogeneous alteration along growth zones with minor dissolution on right edge; (C) Largely unaltered core with large zircon overgrowth; (D) Heterogeneous altered zircon with xenotime overgrowths; (E) Small unaltered euhedral zircon; (F) Homogeneous alteration of growth zones in the core area with larger area of heterogeneous alteration in surrounding area; (G) Porous zircon with patches of heterogeneous alteration; (H) Porous chemically unmodified zircon.
217x296mm (150 x 150 DPI)

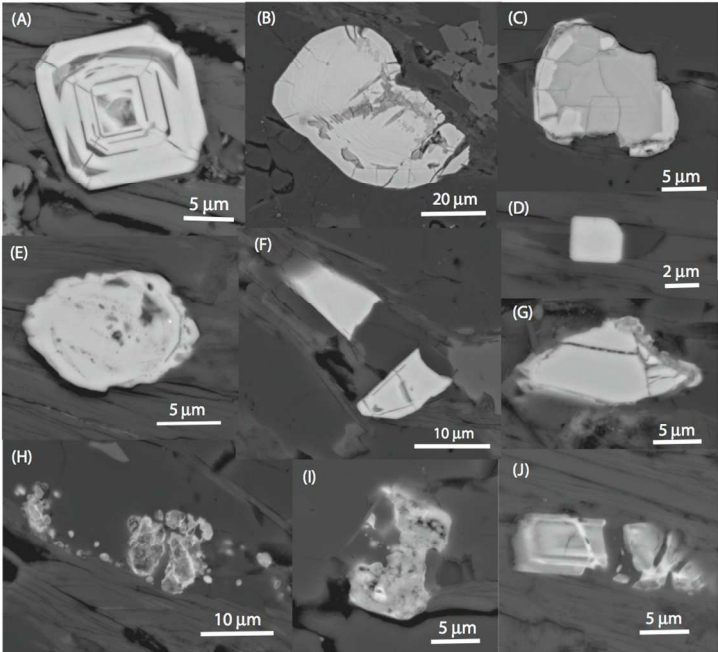


Fig. 4. Representative backscattered electron (BSE) images of zircons from matrix. (A) Homogeneous alteration of internal growth zones; (B) Patchy homogeneous alteration of core area with radial cracking of rim allowing fluid access; (C) Extensive homogeneous alteration; (D) Small unaltered euhedral zircon; (E) Porous zircon with large overgrowths; (F) Fractured zircon with lack of small angular fragments; (G) Largely unaltered zircon with overgrowths; (H) Heterogeneous alteration of zircon with evidence of dissolution (rounding of fragments) and dispersal parallel to rock cleavage; (I) Heterogeneous alteration with large embayments associated with dissolution and replacement by quartz; (J) Homogeneous alteration with evidence of deformation and dissolution.

209x296mm (150 x 150 DPI)

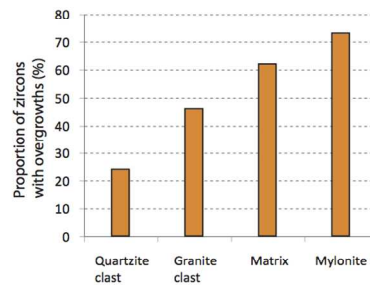


Fig. 5. Histogram showing the proportion of zircons with overgrowths in each lithology.
209x296mm (150 x 150 DPI)

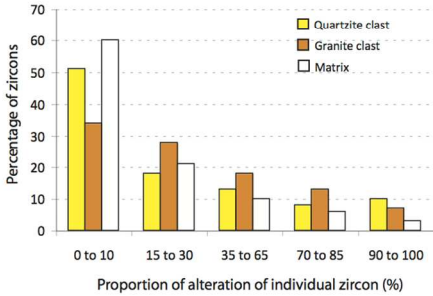


Fig. 6. Histogram showing the amount of alteration of zircon in different host lithologies.
209x296mm (150 x 150 DPI)

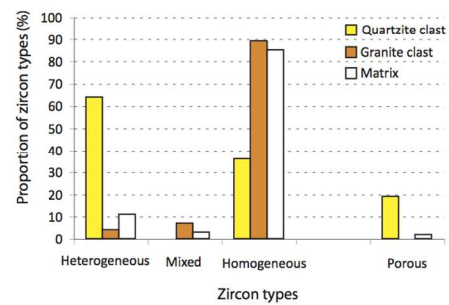


Fig. 7. Histogram showing the proportions of different altered zircon types within each lithology.
209x296mm (150 x 150 DPI)

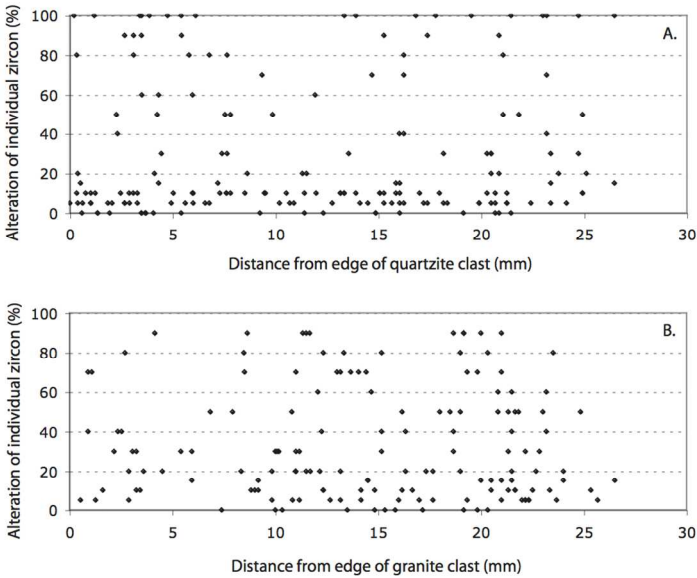


Fig. 8. Plots showing relationship between the amount of alteration in individual zircon grains and their proximity to the clast margin for A. Quartzite clasts and B. Granite clasts.
209x296mm (150 x 150 DPI)

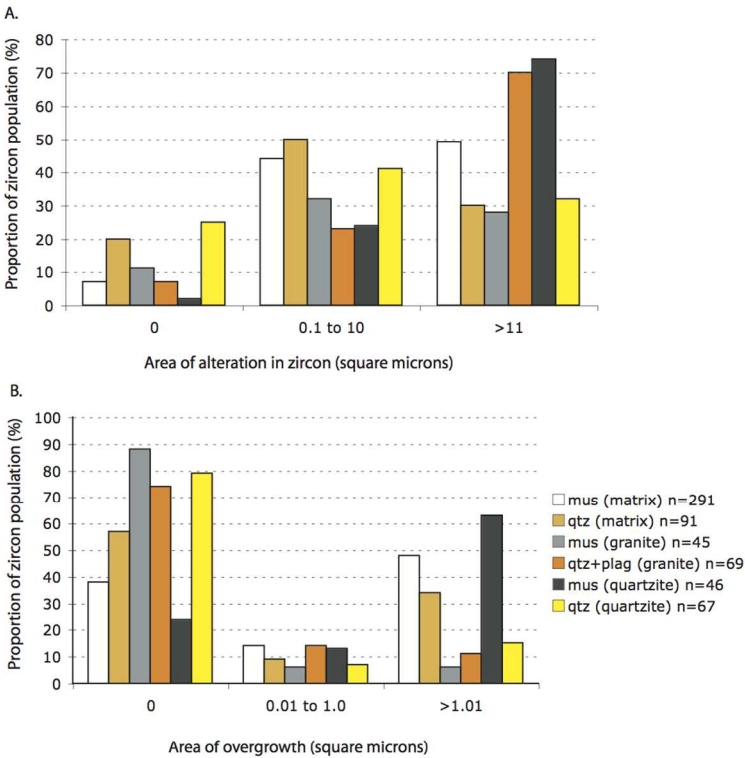


Fig. 9. Histograms showing the influence of adjacent mineralogy on A. the area of alteration in the zircon and B. the area of overgrowth around the zircon.
209x296mm (150 x 150 DPI)

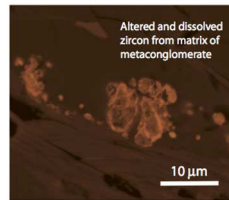
1
2
3
4
5
6
7
8
9
10
11
12
13
14
15
16
17
18
19
20
21
22
23
24
25
26
27
28
29
30
31
32
33
34
35
36
37
38
39
40
41
42
43
44
45
46
47
48
49
50
51
52
53
54
55
56
57
58
59
60

**Controls on fluid movement in crustal lithologies: evidence from zircon in
metaconglomerates from Shetland**

Tim Dempster*, Fiona Macdonald

Movement of low temperature fluids through rocks causes alteration of zircon
resulting in chemical modification, dissolution and new growth. This investigation of
zircon textures in different clast types and matrix in a metamorphosed conglomerate
reveals different responses of zircon linked to different permeability controls. Fluid
influx in these metamorphic rocks is shown to primarily occur along discrete
pathways controlled by the response of quartz, plagioclase and phyllosilicates to
deformation.

Draft Copy



Backscattered electron image of altered zircon
209x296mm (150 x 150 DPI)